Institut Physique de l'Univers
Aix*Marseille Université

Cosmology with Large Scale Structures

Cosmology Team / Christian Marinoni

GECO Team / Eric Jullo

Renoir Team / Dominique Fouchez

Context of the project: Large-scale structure formation?

eBOSS collaboration, 2020

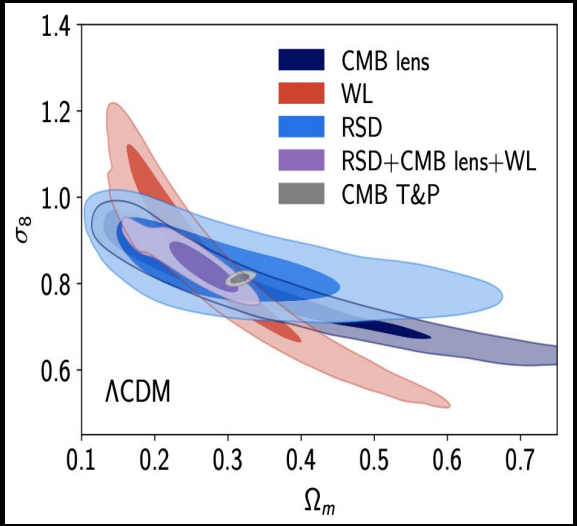

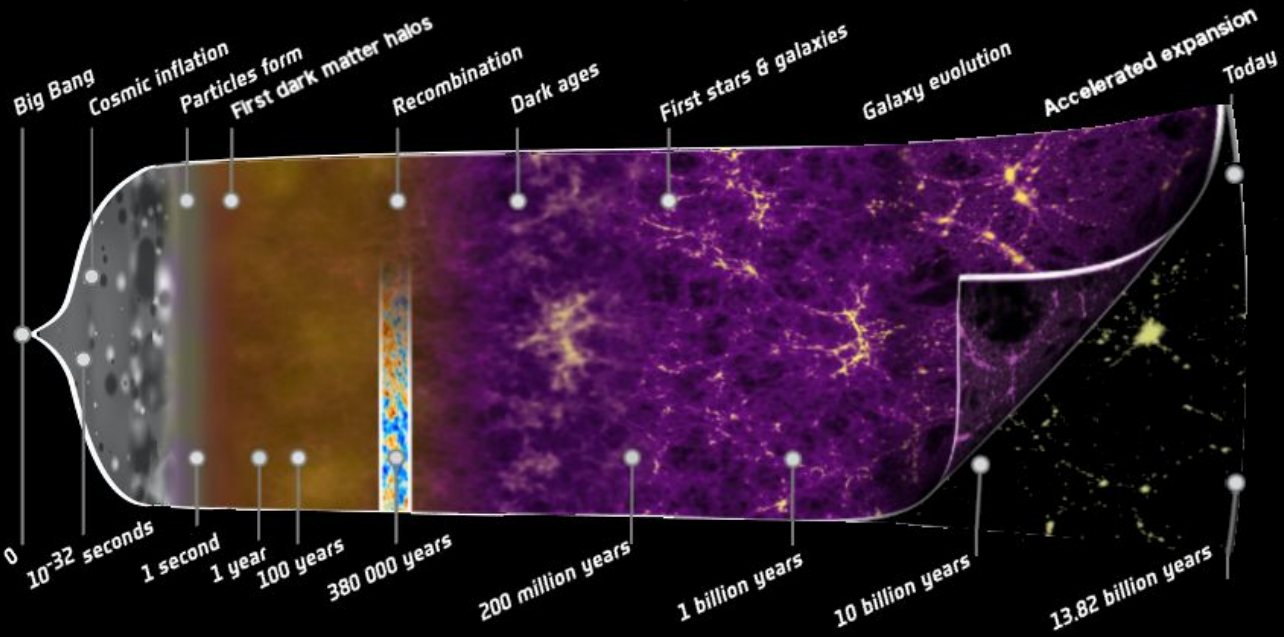

Context: Exquisite precision required <1%

Measure the growth of structure

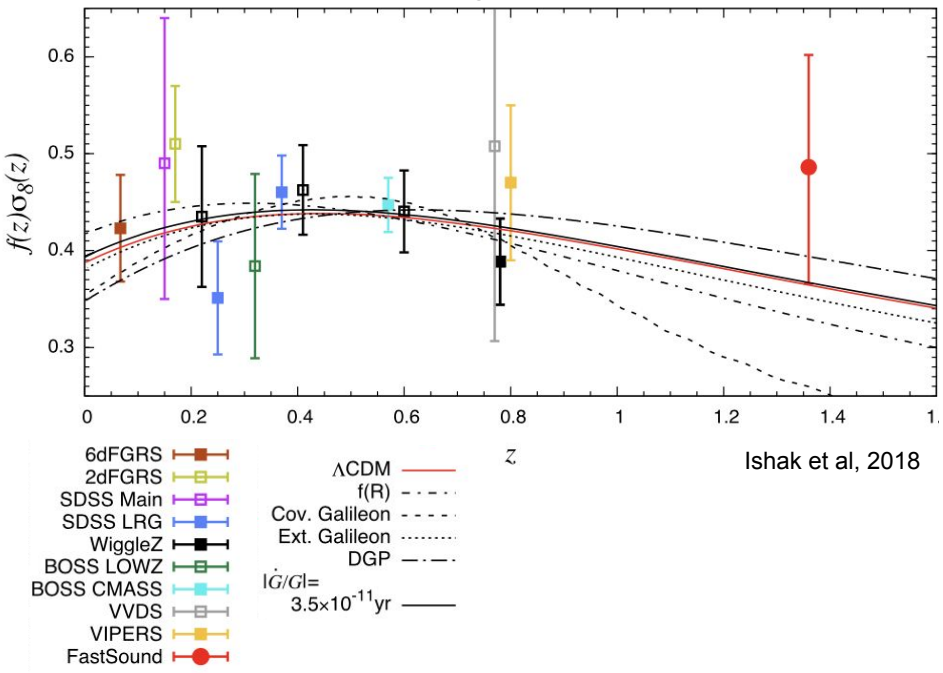

Ishak et al, 2018

Characterize the dark energy EoS

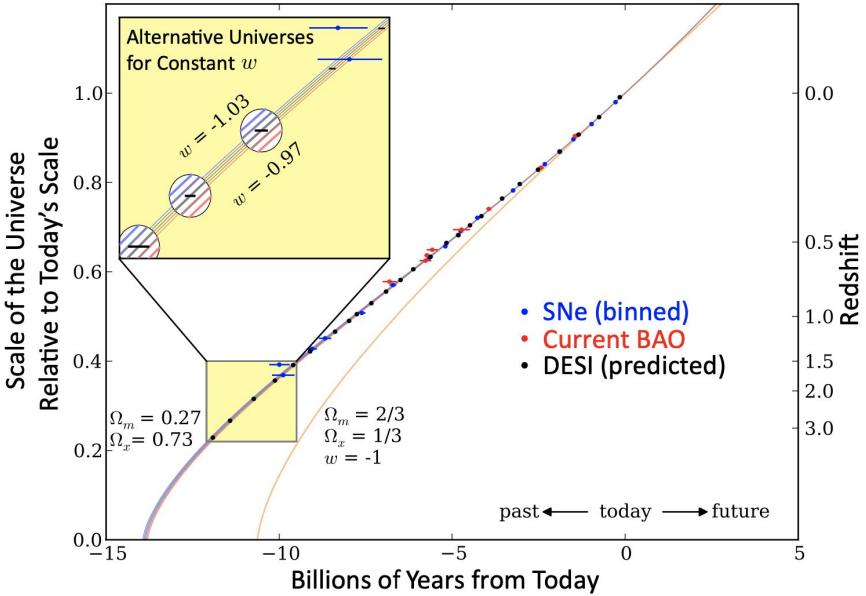

DESI CDR, 2014

Context: Spectroscopic and Photometric surveys

Spectroscopic survey footprint

Credit: C Blake, 2019

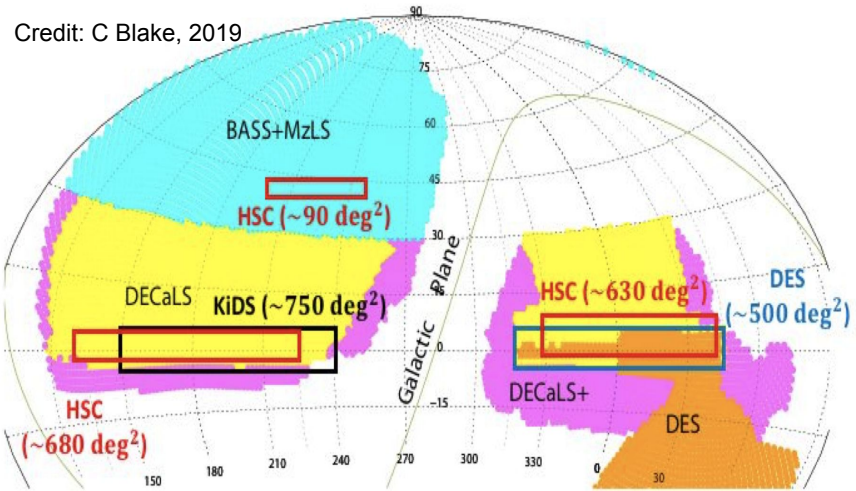

- DESI 14,000deg^2 based on BASS, MzLS, DECaLS, DES imaging
- PFS 1,400 deg^2 in the 3 HSC footprints
- WEAVE-QSO will observe 400,000 spectra in 6,000deg^2 in the SDSS footprint
- GOYA survey will observe high-redshift galaxies behind galaxy clusters

Photometric survey footprint

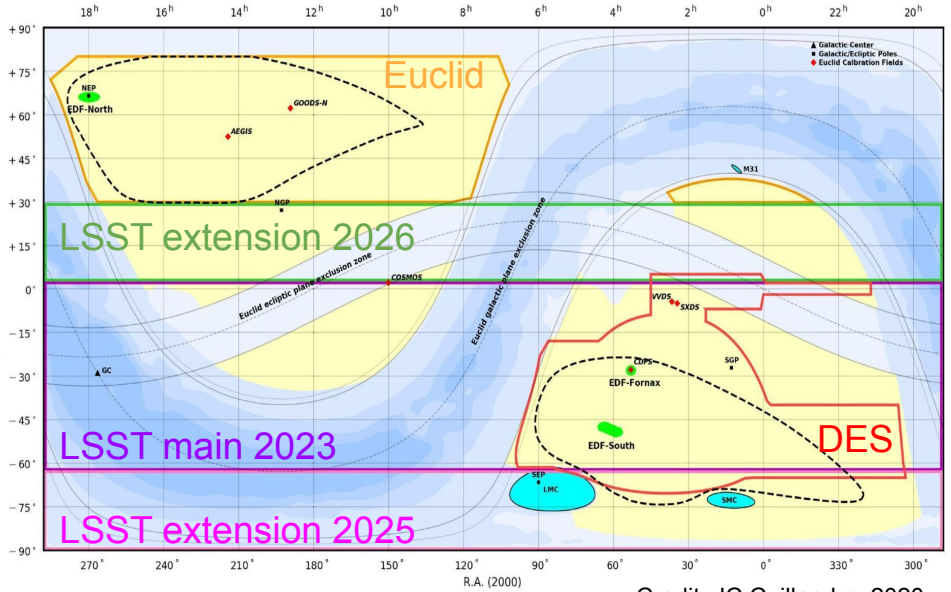

Credit: JC Cuillandre, 2020

- Euclid will observe 15,000deg^2
- LSST will observe 12,000deg^2

Objectives of the project

Characterize dark energy in terms of **cosmic web growth** and **galaxy arrangement**

- Precision cosmology: Dark Energy and Dark matter
  - Theoretical developments on Dark energy
  - Development of cosmological simulations
  - Dark energy constants from the last-scale structure: observational prospects
  - Dark energy and modified gravity constraints from standard candles/sirens
- Cosmic web mapping and galaxy formation
  - First galaxy structures ($3 < z < 7$)
  - Intergalactic medium tomography ($2 < z < 4$)
  - Late time evolution of the cosmic web ($0 < z < 2$)

Roadmap

Surveys	Start [- End]	Surveys	Expected start
eBOSS	2015 - 2019	WEAVE	2020
GOYA/EMIR	2018 - 2023	PFS	2022
DESI	2020 - 2025	Euclid	2022
HSC-CLAUDS	2016-2021	LSST	2022

- **eBOSS:** Cosmological papers published eBOSS collaboration et al. , Press Release July 2020
- **EMIR**: Technical issues. New detectors planned end of 2021. Survey starting 2021 (degraded mode) and end 2023
- **DESI:** 47h SV observations in Dec 2021 (>50k redshifts). Lensing+clustering+void mock challenge
- **HSC-CLAUDS:** Data acquired. On-going analysis on bright and faint galaxy evolution measurements up to z = 3 (Moutard et al. 2020)
- **WEAVE-QSO:** Science observations start Jan 2021
- **PFS:** Integration of 2nd & 3rd spectrographs at LAM. Paper on galaxy emission line models Saito et al. 2020
- **Euclid:** NISP & VIS being integrated on spacecraft. Scientific preparatory work & papers
- **LSST:** 3200 megapixels camera took first image (Sept 2020). Scientific preparatory work & papers

Collaborative Science Aspects

GECO/Cafe club : 28 talks in 2020

CLASS first telecon on June 30th, 2020

- ➢ Need to plan another telecon 1st semester 2021

Wiki page: https://projets.lam.fr/projects/class/wiki

Regular meetings between CPPM, LAM and CPT

Project Setup

Fall 2020 Recruitement of Renan Boschetti, PhD on “voids lensing”

Fall 2020 Recruitement of Reda Ait-Ouahmed, PhD on Deep Learning

New members

- Katarina Kraljic postdoc on cosmic web analysis
- Julian Bautista postdoc on supernovae analysis
- Lucie Khlat PhD on cosmological probes WL+RSD to test gravity
- Bastien Carreres PhD on testing gravity with supernovae

Production of the CLASS project

- Precision cosmology: dark energy & dark matter
  - Theoretical developments on dark energy
  - Developments in cosmological simulations
  - Dark energy constraints from large-scale structures
  - Dark energy & modified gravity constraints from standard candels / sirens
- Cosmic web mapping
  - First galaxy structures ($3 < z < 7$)
  - Intergalactic medium tomography ($2 < z < 4$)
  - Late-time evolution of the cosmic web ($0 < z < 2$)

PhD on void lensing as a test of gravity

Renan Boschetti, Marie Aubert, Marie-Claude Cousinou, Stéphanie Escoffier, Eric Jullo

Why void lensing?

- Voids have a huge potential to constrain gravitational fifth forces and dark energy
- Gravitational lensing is a direct probe of matter
- Void Lensing has been detected in the DES-Y1 and SDSS

=> Work started on DESI simulated data of LRG & BGS

=> Regular telecon with the DESI C^3 WG

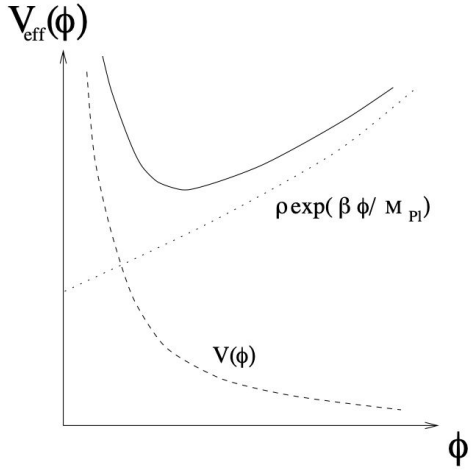

The effective potential is the sum of a scalar dependent potential, and a density dependent potential (Khoury & Weltman, 2003)

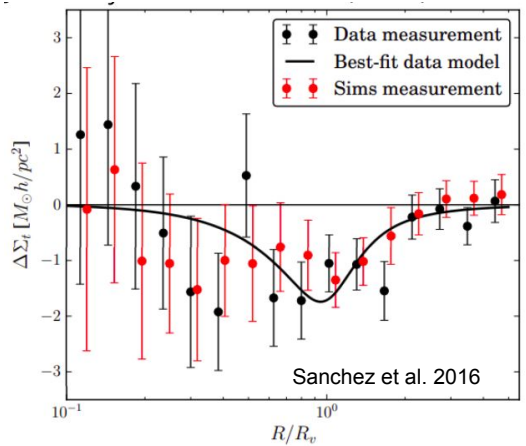

extended Fast Action Minimisation method: application to SDSS-DR12 Combined Sample

E. Sarpa,[1,2,3]★ A. Veropalumbo,[2,3] C. Schimd,[1] E. Branchini,[2,3,4] S. Matarrese.[5,6,7,8]

[1] *Aix Marseille Univ, CNRS, CNES, LAM, Marseille, France*
[2] *Dipartimento di Matematica e Fisica, Università degli studi Roma Tre, Via della Vasca Navale, 84, 00146 Roma, Italy*
[3] *INFN - Sezione di Roma Tre, via della Vasca Navale 84, I-00146 Roma, Italy*
[4] *INAF - Osservatorio Astronomico di Roma, via Frascati 33, I-00040 Monte Porzio Catone (RM), Italy*
[5] *Dipartimento di Fisica e Astronomia "Galileo Galilei", Università degli studi di Padova, Via F. Marzolo, 8, I-35131 Padova, Italy*

arXiv:2010.10456
MNRAS, accepted

ABSTRACT

We present the first application of the extended Fast Action Minimization method (eFAM) to a real dataset, the SDSS-DR12 Combined Sample, to reconstruct galaxies orbits back-in-time, their two-point correlation function (2PCF) in real-space, and enhance the baryon acoustic oscillation (BAO) peak. For this purpose, we introduce a new implementation of eFAM that accounts for selection effects, survey footprint, and galaxy bias. [*abridged*]

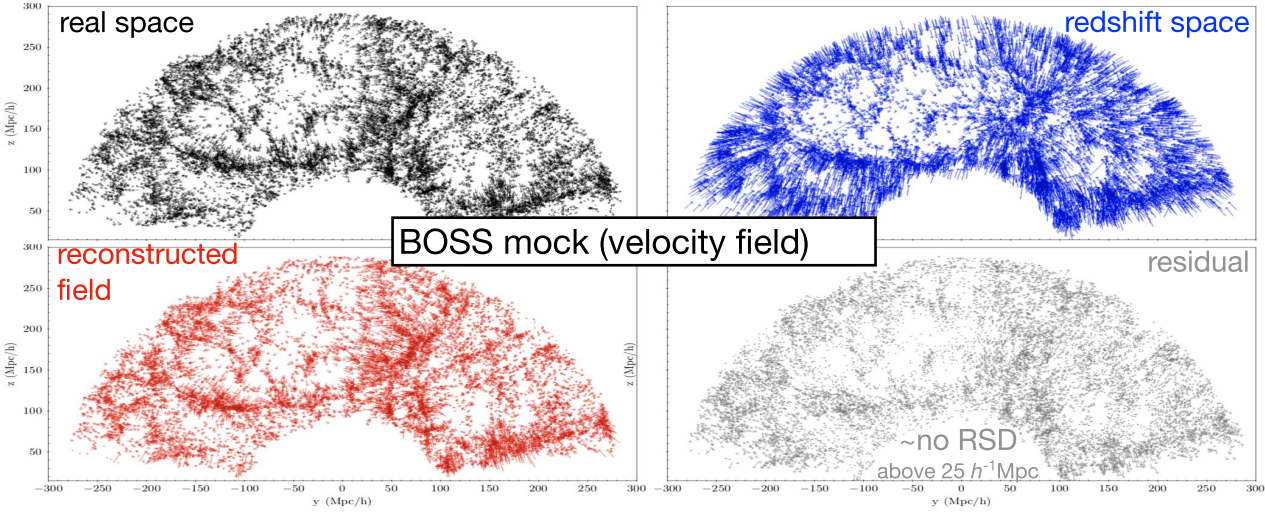

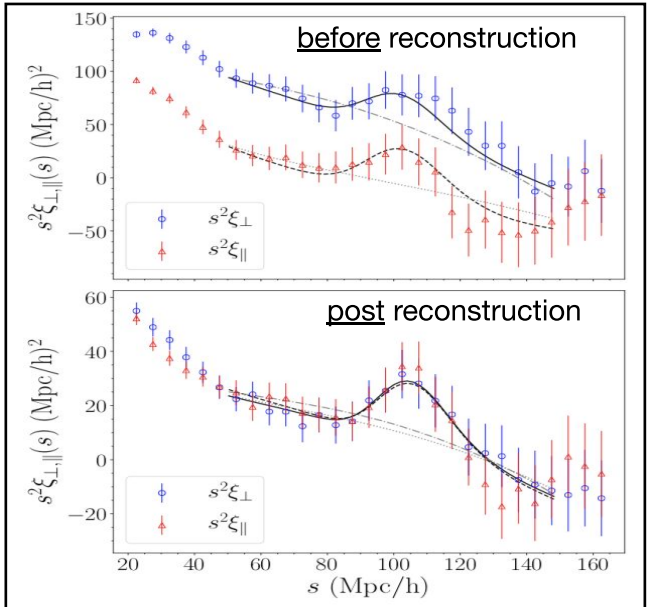

Figure 9. Clustering wedges of the BOSS-DR12 Combined Sample before (top-panel), and after eFAM reconstruction (bottom-panel). Open blue circles show the measured perpendicular wedge. Open red triangles show the parallel wedge. The error-bars are the square root of diagonal of the covariance matrix estimated from the mocks. Best fit clustering wedges models are also shown with black continuous curves. Solid and dashed curves show the best fit model that include the BAO feature. Dot and dot-dashed curves are best fitting models with no acoustic peak.

improvements: **(1)** BAO angular distance: 3.6% (pre-rec) ➠ 2.3% (post-rec) **(2)** 2PCF reconstructed down to ~25 h^{-1}Mpc, reducing RSD **(3)** reduced AP uncertainties by 40%

High-precision Monte Carlo modelling of galaxy distribution

Philippe Baratta[1,2], Julien Bel[2], Stephane Plaszczynski[3], and Anne Ealet[1,4]

[1] Aix Marseille Université, CNRS/IN2P3, CPPM, Marseille, France
e-mail: baratta@cppm.in2p3.fr
[2] Aix Marseille Univ, Université de Toulon, CNRS, CPT, Marseille, France
[3] LAL, Univ. Paris-Sud, CNRS/IN2P3, Université Paris-Saclay, Orsay, France
[4] Institut de Physique Nucléaire de Lyon, 69622 Villeurbanne, France

arXiv 1906.09042

—> Proposing a method allowing to generate a non-Gaussian density field with arbitrary matter power spectrum and probability distribution function (analytical or numerical) at a given redshift
—> Discretising this continuous field (to get galaxies, dark matter particles, halos, etc) by introducing several interpolation schemes
—> Introducing some light-cone reconstruction methods
—> Can be applied in order to estimate the P(k) or the Cl covariance matrix for galaxy clustering (but can be extended to other probes)

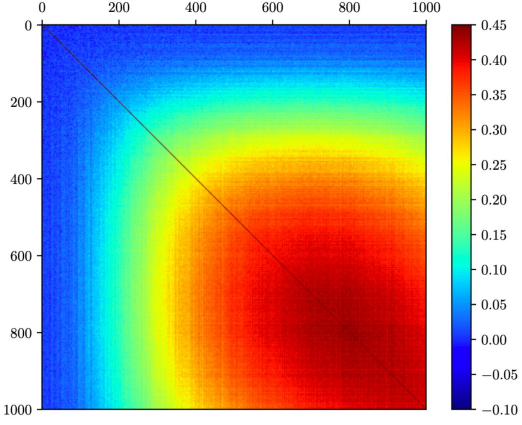

Fig. 15. Correlation matrix for 10 000 realisations of C_ℓ in a simulated universe between redshifts 0.2 and 0.3 and a sampling $N_s = 512$. The $(\ell \times \ell') = (1000 \times 1000)$ of the matrix are represented here.

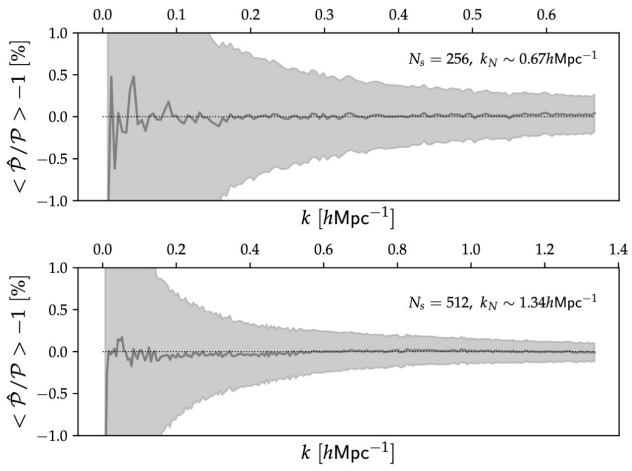

Fig. 6. Averaged 3D power spectrum compared to the expected 3D power spectrum, for 1000 realisations of the density field. The shell-averaged monopoles of this residuals in shells of width $|\boldsymbol{k}|-k_f/2 < |\boldsymbol{k}| < |\boldsymbol{k}|+k_f/2$ were then computed. The result is presented as percentage with error bars. The setting used is a sampling number per side of 256 in the *top panel* and 512 for the other, all in a box of size $L = 1200\,h^{-1}$ Mpc at redshift $z = 0$. Both results are computed up to the Nyquist frequency.

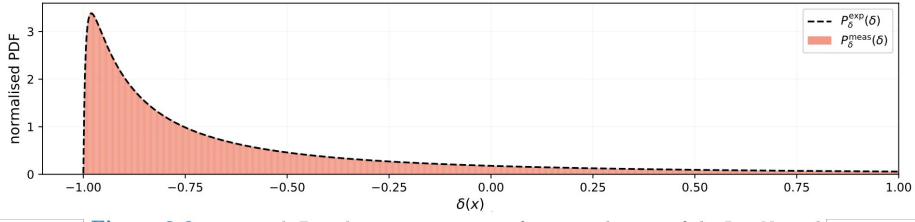

Figure 3.6: *top panel:* Distribution measurement for one realisation of the Log-Normal Monte Carlo field δ (in orange) as compared to its prediction (dashed black line, see eq. 3.18) for the truncated interval $\delta \in [-1, 1]$. *bottom panel:* relative deviation between the two distributions in a wider interval $\delta \in [-1, 10]$.

Cosmological constraints from eBOSS LRG clustering analysis

The Completed SDSS-IV extended Baryon Oscillation Spectroscopic Survey: measurement of the BAO and growth rate of structure of the luminous red galaxy sample from the anisotropic correlation function between redshifts 0.6 and 1

Julian E. Bautista[1⋆], Romain Paviot[2,3†], Mariana Vargas Magaña[4‡], Sylvain de la Torre[2], Sebastien Fromenteau[5], Hector Gil-Marín[6,7], Ashley J. Ross[8], Etienne Burtin[9], Kyle S. Dawson[10], Jiamin Hou[11], Jean-Paul Kneib[12], Arnaud de Mattia[9], Will J. Percival[13,14,15], Graziano Rossi[16], Rita Tojeiro[17], Cheng Zhao[12], Gong-Bo Zhao[18,19,1], Shadab Alam[20], Joel Brownstein[10], Michael J. Chapman[13,14], Peter D. Choi[16], Chia-Hsun Chuang[21], Stéphanie Escoffier[3], Axel de la Macorra[4], Hélion du Mas des Bourboux[10], Faizan G. Mohammad[13,14], Jeongin Moon[16], Eva-Maria Müller[22], Seshadri Nadathur[1], Jeffrey A. Newman[23], Donald Schneider[24,25], Hee-Jong Seo[26], Yuting Wang[18]

from arXiv:2007.08991

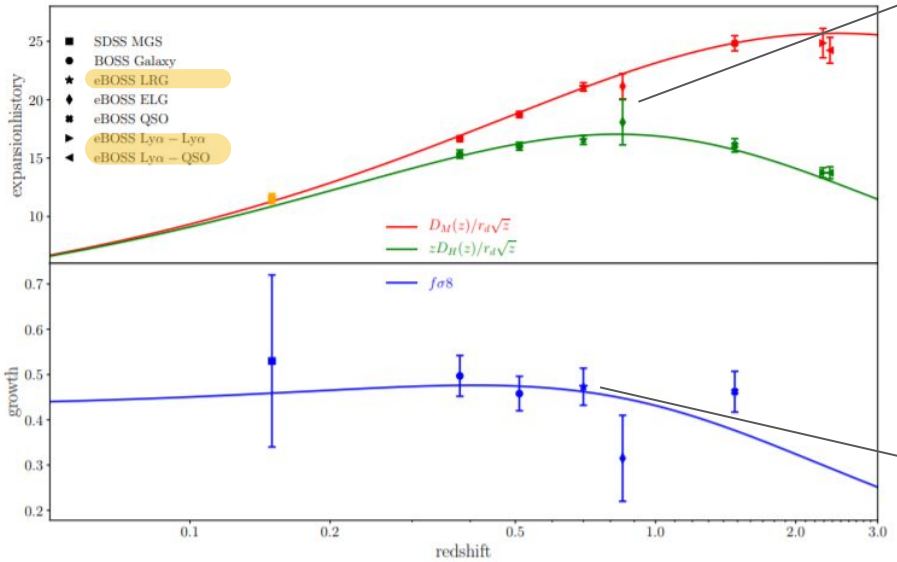

LRG

LRG

Table 14. Summary table with results from this work, from Gil-Marín et al. (2020), and their combination. All reported errors include the systematic component. The effective redshift of all measurements is $z_{\rm eff} = 0.698$.

Method	D_M/r_d	D_H/r_d	$f\sigma_8$
BAO ξ_ℓ	17.86 ± 0.33	19.34 ± 0.54	-
BAO P_ℓ	17.86 ± 0.37	19.30 ± 0.56	-
BAO $\xi_\ell + P_\ell$	17.86 ± 0.33	19.33 ± 0.53	-
RSD ξ_ℓ CLPT	17.39 ± 0.43	20.46 ± 0.68	0.471 ± 0.052
RSD ξ_ℓ TNS	17.45 ± 0.38	20.45 ± 0.72	0.451 ± 0.047
RSD ξ_ℓ	17.42 ± 0.40	20.46 ± 0.70	0.460 ± 0.050
RSD P_ℓ	17.49 ± 0.52	20.18 ± 0.78	0.454 ± 0.046
RSD $\xi_\ell + P_\ell$	17.40 ± 0.39	20.37 ± 0.68	0.449 ± 0.044
BAO+RSD ξ_ℓ	17.65 ± 0.31	19.81 ± 0.47	0.483 ± 0.047
BAO+RSD P_ℓ	17.72 ± 0.34	19.58 ± 0.50	0.474 ± 0.042
BAO $(\xi_\ell + P_\ell)$ + RSD $(\xi_\ell + P_\ell)$	17.65 ± 0.30	19.77 ± 0.47	0.473 ± 0.044
(BAO+RSD) ξ_ℓ + (BAO+RSD) P_ℓ	17.64 ± 0.30	19.78 ± 0.46	0.470 ± 0.044

Testing general relativity with type Ia supernovae peculiar velocities

Bastien Carreres, Julian Bautista, Dominique Fouchez, Benjamin Racine, Fabrice Feinstein

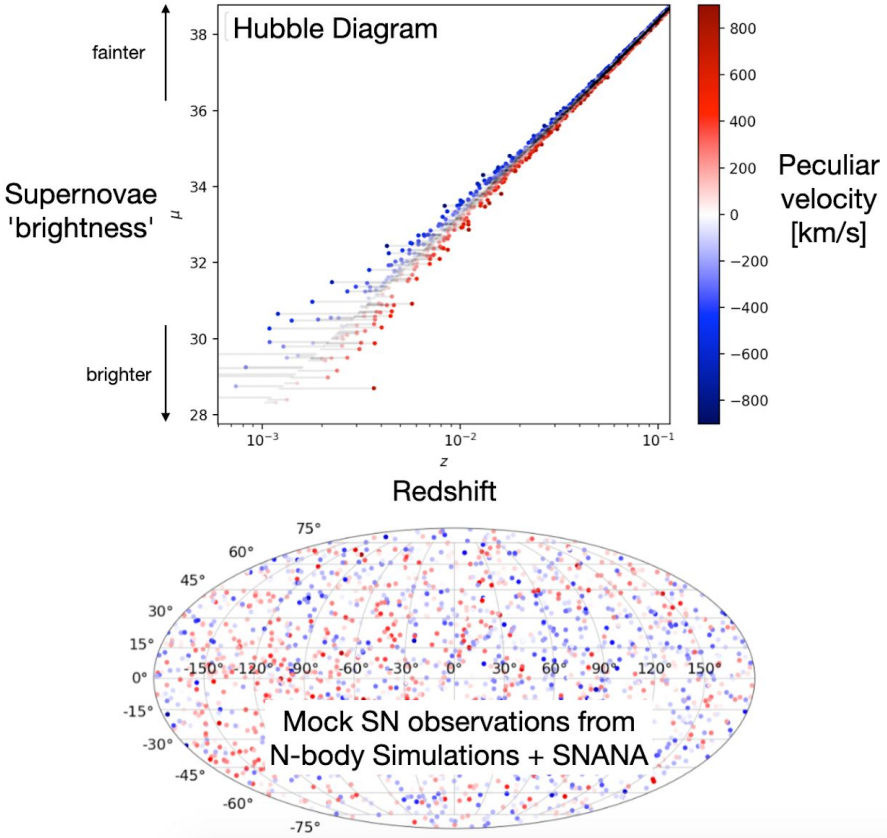

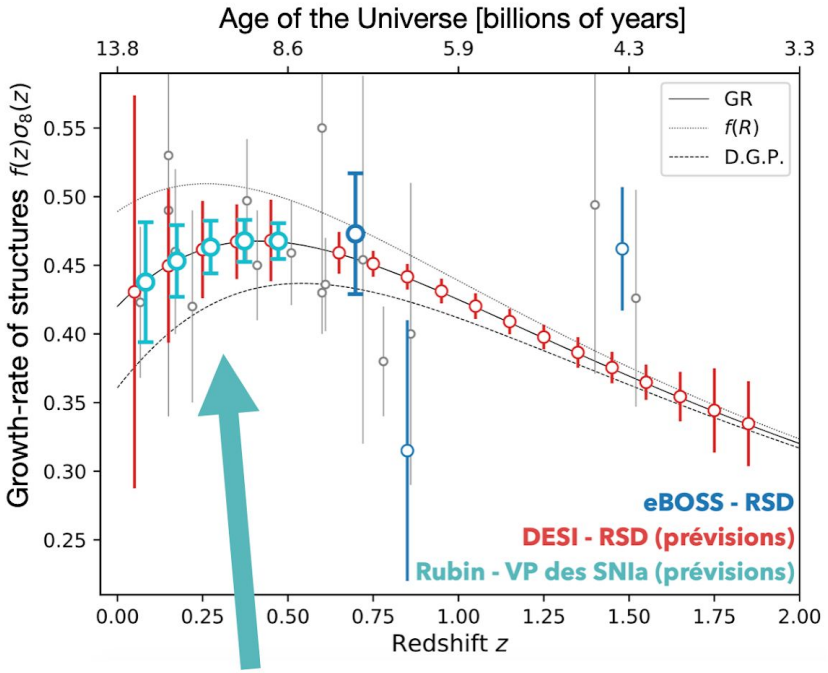

Peculiar velocities with SNIa from ZTF and **Rubin Observatory** will be the best probe of gravity on large-scales at low redshift (Howlett et al. 2017, Graziani et al. 2020)

Constraints on the growth rate of structure with voids in the eBOSS DR16 ELG, LRG and QSO samples with voids

The Completed SDSS-IV Extended Baryon Oscillation Spectroscopic Survey: Growth rate of structure measurement from cosmic voids

Marie Aubert[1]*, Marie-Claude Cousinou[1], Stéphanie Escoffier[1], Adam J. Hawken[1], Seshadri Nadathur[2], Shadab Alam[3], Julian Bautista[2], Etienne Burtin[4], Chia-Hsun Chuang[5], Arnaud de Mattia[4], Héctor Gil-Marín[6,7] Jiamin Hou[8], Eric Jullo[9], Jean-Paul Kneib[10], Richard Neveux[4], Graziano Rossi[11], Alex Smith[4], Amélie Tamone[10], Mariana Vargas Magaña[12], Cheng Zhao[10]

Arxiv:2007.092013
submitted to MNRAS.

Table 9. Final results on the growth rate estimate from the eBOSS DR16 void datasets. Mean values and errors on β are taken from Table 8. The presented errors include the systematic component. The reported value of $b_1\sigma_8$ are taken from clustering analysis in the DR16 companion papers, for the LRG+CMASS sample (Bautista et al. 2020; Gil-Marin et al. 2020), the ELG sample (Tamone et al. 2020; De Mattia et al. 2020) and the QSO sample (Hou et al. 2020; Neveux et al. 2020). The growth rate constraint results from applying Eq. 36 to these values. The total error quoted for $f\sigma_8$ includes the galaxy bias error contribution.

Data samples	$z_{\rm eff}$	β	$b_1\sigma_8$	$f\sigma_8$
LRG+CMASS	0.740	0.415 ± 0.087	1.20 ± 0.05	0.50 ± 0.11
ELG	0.847	0.665 ± 0.125	0.78 ± 0.05	0.52 ± 0.10
QSO	1.478	0.313 ± 0.134	0.96 ± 0.04	0.30 ± 0.13

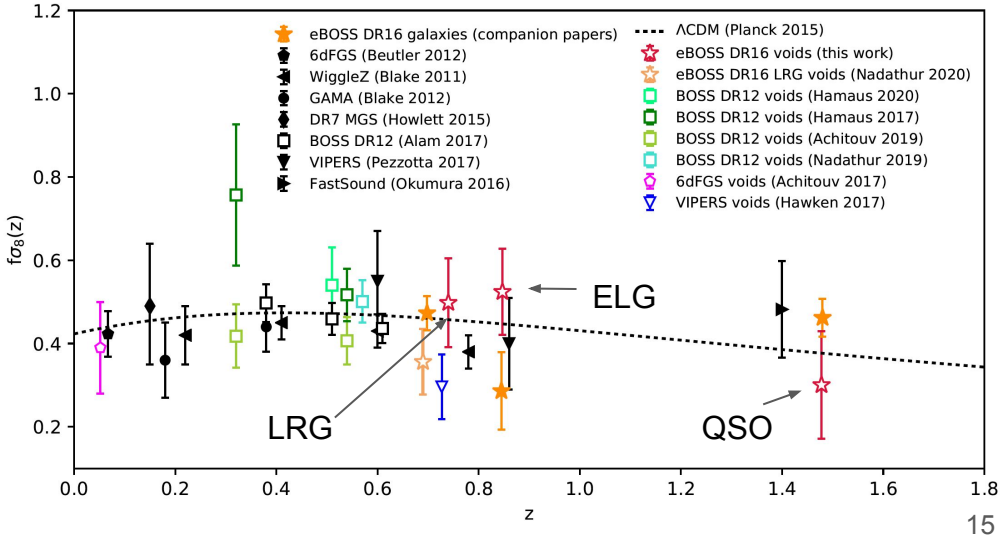

First galaxy structure : Lyα Emitters vs Ly Break Galaxies

de la Vieuville, Pelló et al. 2020

Blind selection of Lyα Emitters (LAE) at 2.9 < z < 6.7 with **MUSE/VLT** behind A2744: Complete census of Star Forming galaxies at the epoch of the reionization

- Detection of a LAE population with intrinsically UV faint flux (M(1500A) ≥ −15) with significant star-formation (typically 0.01 to 0.1 M⊙/yr) that are missed in the deepest LBG surveys.
- As faint as M(1500A) ~ −15, the LBG population provides a good representation of the total Star Forming Galaxy population, in particular when computing the total ionizing flux in the volume explored by current surveys.

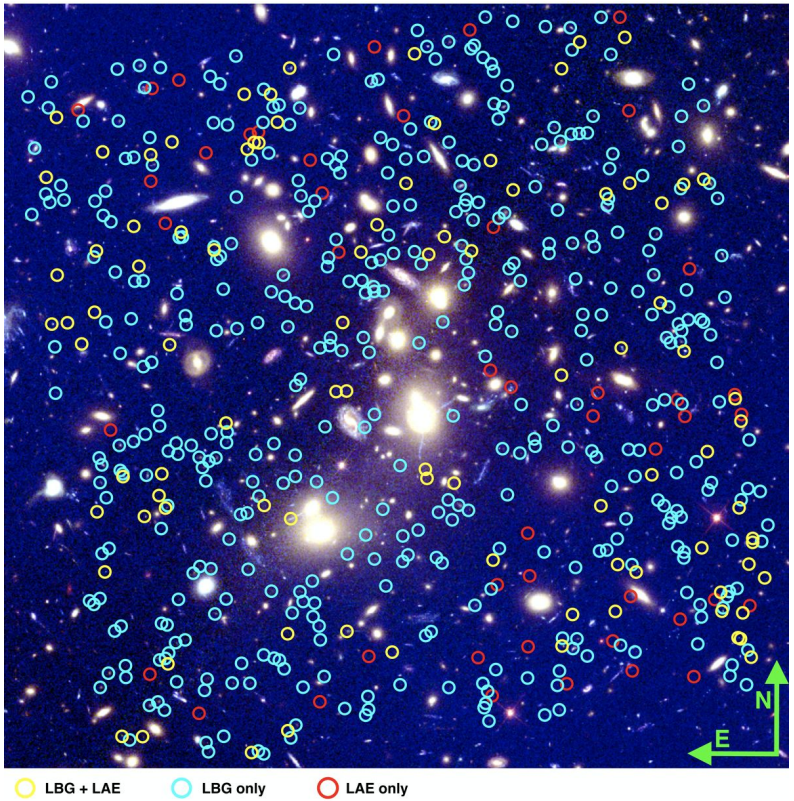

Probing Large-scale UV Background Inhomogeneity Associated with Quasars using Metal Absorption

Sean Morrison,[1]★ Matthew M. Pieri,[1]† Debopam Som,[1,2,3] and Ignasi Pérez-Ràfols[1,4]

- Probing the UV background using quasar absorption in SDSS (arXiv:2012.00772)
- Metal species dependence on quasar proximity detected (~5σ)
  - scales much larger than previously thought (~10 cMpc/h)
  - consistent with initial findings of Morrison et al (2019) using HST+VLT spectra
- Potential consequences for
  - reionization and maintaining ionization
  - measurements of BAO using quasar absorption

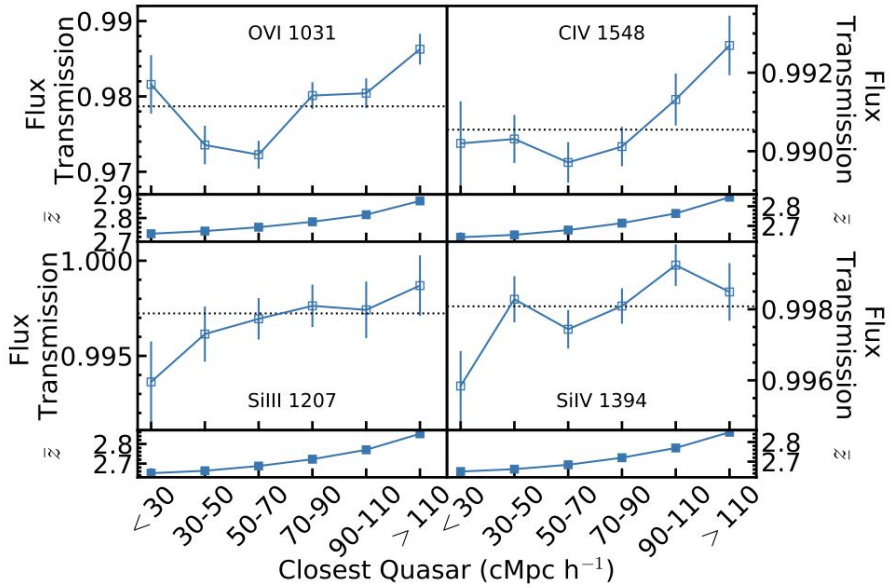

Conclusion

A lot of activity within the group in 2020

We acknowledge the financial support from OCEVU and IPhU

With forthcoming data, many systematic errors, and new physical effects must/can be taken into account. This is an exciting period of time.

Galaxy evolution in the cosmic web has a growing impact on cosmological studies on dark matter, dark energy and modified gravity => need to strengthen this aspect

Probing dark energy with weak lensing mass maps

- Weak lensing mass maps (including peaks and voids) probe the non-Gaussian part of the matter distribution, bringing complementary information to standard 2-point estimators
- We developed a new tomographic approach of mass maps, and showed that it improves Euclid forecasts on the dark energy equation of state w by a factor of 3 compared to the standard shear two-point correlation functions implemented in Euclid (Martinet, Harnois-Deraps, Jullo et al. 2020a, https://arxiv.org/abs/2010.07376)
- We measured the impact of baryons on mass map statistics and found that the AGN feedback from the Magneticum hydrodynamical simulation propagates into a few percent bias on w for Euclid forecast and will need to be accounted for (Martinet et al. 2020b, https://arxiv.org/abs/2012.09614)
- We applied tomographic mass maps to the DES-Y1 1300 deg2 survey accounting for all sources of biases and get a 4.8% precision on the structure growth parameter S8. The full tomographic approach reaches a 3% precision but could not be implemented due to a lack of understanding of intrinsic alignments in this case. The probed area does not allow us to constrain w yet. (Harnois-Deraps, Martinet et al. 2020, https://arxiv.org/abs/2012.02777)

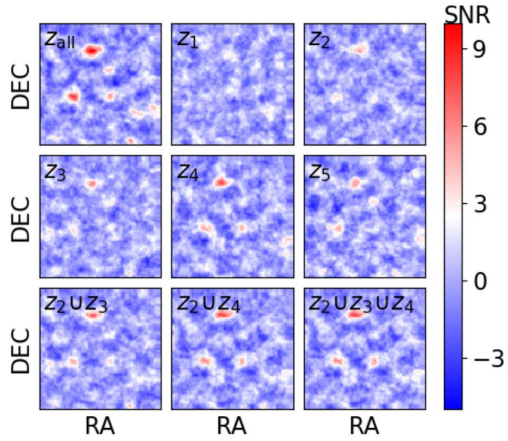

Tomographic mass map reconstruction

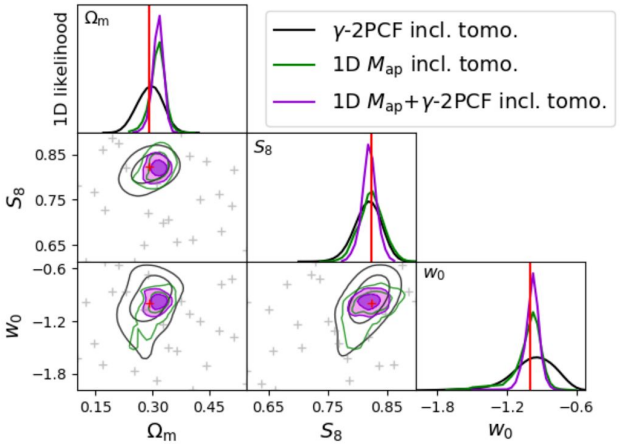

Euclid forecasts *(100 deg2) for mass maps (1D Map) and shear two point correlation functions (2PCF)*